EMAE TR 96-216

Evidence for Transient Disturbance Growth in a 1961 Pipe-Flow Experiment

Ernst W. Mayer

and

Eli Reshotko

Department of Mechanical and Aerospace Engineering
Case Western Reserve University
Cleveland, Ohio 44106

1996

Evidence for transient disturbance growth in a 1961 pipe-flow experiment

Ernst W. Mayer and Eli Reshotko
Department of Mechanical & Aerospace Engineering, Case Western Reserve University
10900 Euclid Avenue, Cleveland, OH 44106-7222 *

August 12, 1996

Evidence is presented for what appears to have been non-modal disturbance growth in a pipe-flow experiment performed by Kaskel [1] in 1961, based on a comparison of the experimental traces of disturbance amplitude with predictions of transient amplitude growth calculated from the underlying linear stability operator. Owing to the geometry of the experimental disturbance generator, modes having azimuthal wavenumbers $n = 0$, 6 and 12 are expected to contribute the bulk of the disturbance energy, and the corresponding numerical predictions of amplitude growth versus time and downstream distance are in good agreement with the experiment.

It has recently emerged [2, 3, 4, 5, 6, 7] that in many fluid flows, even in those which have no exponentially growing modes according to classical linear stability theory, significant non-modal transient disturbance growth may occur if the underlying differential stability operator is non-normal, i.e. has nonorthogonal eigenfunctions. There is a growing body of evidence that such non-modal growth is an important component of so-called bypass transition in channel and boundary-layer flows, as well as in the short-time behavior of disturbances on flows which *do* have classically unstable eigenmodes. Klingmann [8], in her experimental study of the growth of point-like disturbances in channel flow at subcritical Reynolds numbers, observed evolution of the initial disturbance into elongated streaky structures having strong spanwise shear, in good agreement with the predictions of three- dimensional non-modal linear theory. For circular-pipe flow, Bergström [9, 10] experimentally investigated the evolution of both point-like and non-axisymmetric distributed disturbances in a water-pipe system and found qualitative agreement with the predictions of non-modal growth theory, although the axially localized pulses produced by his disturbance generator imply that modes having all possible axial wavenumbers are simultaneously present, precluding a direct comparison with the theoretical predictions. In another set of studies, O'Sullivan & Breuer [11, 12] studied linear and nonlinear disturbance evolution via spectral-numerical techniques and a carefully chosen

*E-mail: *mayer@nigel.mae.cwru.edu, exr3@po.cwru.edu*

variety of initial disturbance states, and found short-time disturbance amplification in good accord with the theoretical predictions of Schmid & Henningson [7] and both linear and nonlinear development in agreement with theoretical predictions for long-wave evolution of Bergström [13, 14, 15].

While Kaskel's experimental data do not contain the level of detail which one would like for a complete comparison with the theory, the description of the experimental apparatus, in particular the disturbance generator, allows for a reasonably good estimation of the structure of the initial disturbance field (i.e. the relative amplitudes of components having different azimuthal wavenumbers). These data, when combined with the disturbance growth data from linear non-modal theory, yield predictions of amplitude growth which can be compared with the experimental traces of disturbance amplitude evolution. Interestingly, due to the structure imposed on the initial disturbance field, it is not the low-order asymmetric helical modes found by Schmid & Henningson and Bergström to have the greatest growth potential which dominate the growth in Kaskel's experiment; rather, the amplitude evolution is dominated by the axisymmetric ($n = 0$) modes, with smaller contributions from the $n = 6$ and $n = 12$ mode families.

The establishment of the undisturbed axisymmetric Poiseuille flow in a 2 in. ID pipe which served as the base flow for the experiment is described in detail by Reshotko [16]. With a proper choice of inlet section and a thorough cleaning of the inside walls of the system, laminar flow was observed at Reynolds numbers up to 23,000. For $Re = 7,600$, the Reynolds number at which the disturbance measurements were made by Kaskel, the flow was symmetric to better than 2%.

The disturbance generator which was used in the experiments is described in detail by Kaskel [1]. It consisted of a pipe section containing six cantilevered, magnetically vibrated reeds equally spaced about the outer circumference. An electronic oscillator was used to vibrate the reeds at a known frequency and amplitude, and a hot-wire probe mounted on a precision traversing mechanism was used to measure downstream flow velocities and disturbance amplitudes. Axial traverses were used to measure the amplitude and phase evolution of disturbances at frequencies of f = 3, 5, 10 and 15 Hz. We focus our attention only on the 10 Hz and 15 Hz measurements, for which disturbance wavelengths (5.59 in. and 3.60 in.) and phase velocities (55.9 in/sec. and 54.0 in/sec.) were accurately measurable, allowing one to infer the axial disturbance wavenumber, using the relation

$$\alpha = \frac{2\pi}{\lambda} = \frac{2\pi f}{f\lambda} = \frac{2\pi f}{C_{ph}}. \tag{1}$$

The 10 Hz and 15 Hz disturbances are thus found to have nondimensional axial wavenumbers $\alpha = 1.12$ and $\alpha = 1.75$, respectively[a].

The corresponding traces of disturbance amplitude (measured at the radial location where the largest hot-wire output was seen, i.e. within the critical layer) versus axial distance are reproduced in Figures 1 and 2 (the experimental traces are the wiggly lines). At the two frequencies shown, the disturbance amplitude shows a rapid initial rise in which the amplitude increases by a factor of roughly 4 and 3.5, respectively, followed by a smooth decay. Due to the physical limitations of the traversing mechanism, the decay phase is clearly documented down to the experimental noise level only in the 15 Hz case, but in this latter case it clearly resembles an exponential decay.

Once the disturbance parameters of the experiment are established, in order to make a meaningful comparison of the experimental results with the predictions of non-modal disturbance analysis one also needs to (i) estimate the relative initial amplitudes of disturbances having different integer azimuthal wavenumbers in the experiment, and (ii) convert the transient growth estimates resulting from the temporal linear stability calculations into estimates of amplitude as a function of downstream distance. We shall address each of these items, in order.

To estimate the relative amplitudes of axisymmetric and nonaxisymmetric disturbances induced by Kaskel's 6-lobed disturbance generator, we use the fact that the centerline of each lobe moves periodically, rigidly and linearly, with the center of each lobe moving purely radially. Thus the nonradial (i.e. azimuthal) component of the motion induced by the rigidly translating lobe increases from zero as one moves away from the lobe centerline, reaching a maximum at the extreme edges of each lobe. The geometric statement of this, taking the lobe centerlines to be located at $\theta_{1,2,3,4,5,6} = 0, \frac{\pi}{3}, \frac{2\pi}{3}, \pi, \frac{4\pi}{3}, \frac{5\pi}{3}$ and neglecting the small gaps between lobes, is

$$U_r(\theta,t) = U_0(t)\cos(\theta-\theta_j) \text{ for } \theta-\theta_j \in [-\frac{\pi}{6},\frac{\pi}{6}], \qquad j=1,\ldots,6, \tag{2}$$

where $U_0(t)$ is the time-periodic radial velocity of the centerline, which is the same for each lobe since all six lobes vibrated in phase. The azimuthal velocity U_θ induced by the disturbance generator has exactly the same form, but with sines replacing the cosines in the above formula. The azimuthal components of U_r and U_θ can be expanded in a Fourier cosine and sine series, respectively, (having

[a] In the theoretical formulation, all lengths are nondimensionalized by the pipe radius, 1 in., hence λ and α have the same numerical value in dimensional and nondimensional form.

the same coefficients):

$$U_r(\theta,t) = U_0(t)\sum_{n=0}^{\infty} c_n \cos(n\theta), \qquad U_\theta(\theta,t) = U_0(t)\sum_{n=0}^{\infty} c_n \sin(n\theta). \tag{3}$$

Due to the sixfold symmetry of U_r and U_θ, the only nonzero coefficients occur in multiples of six:

$$c_0 = \frac{3}{\pi}, \quad c_6 = \frac{6}{35\pi}, \quad c_{12} = -\frac{6}{143\pi}, \ldots, c_{(6p)} = \frac{(-1)^{p+1}6}{(36p^2-1)\pi}, \tag{4}$$

which of course sum to unity. The fact that terms having mode number larger than 12 contribute less than 1% of the total disturbance amplitude in the above model (once one has factored in the maximum amplitude growth for each azimuthal disturbance wavenumber as given by the non-modal analysis) allows one to truncate the series after the first three nonzero terms without an appreciable loss of accuracy, especially in light of the decreasing non-modal disturbance growth of large-azimuthal-wavenumber disturbances predicted by the numerical calculations.

The conversion of the results of the temporal transient growth theory for comparison with the spatial transient growth observations (i.e. amplitude traces) was accomplished using the experimentally measured phase velocities. The reason we do not solve the spatial problem is that, as discussed in detail in [17], there is as yet no consistent way of formulating the non-modal analysis for the spatial case.

Several authors[7, 11] have done transient-growth computations for pipe Poiseuille flow based on the radial velocity–radial vorticity form of the linear disturbance equations first derived by Burridge & Drazin[18]. This approach is useful in revealing similarities (as well as differences, especially in the coupling terms) between the structure of the pipe-flow stability operator and the Orr-Sommerfeld/Squire system governing planar flows. However, there is no special advantage in the use of this formulation for numerical stability calculations. Here, we use a primitive-variable approach similar to that used by Mayer & Powell [19] to investigate the stability of trailing-line vortex flow. We begin with the viscous linear stability equations that result from assuming normal-mode disturbances of the form

$$[\hat{u},\hat{v},\hat{w},\hat{p}](r) = [iu, v, w, p](r)\exp\{i(\alpha z + n\theta - \omega t)\}, \tag{5}$$

where $\hat{u}$, $\hat{v}$ and $\hat{w}$ are the radial, azimuthal and axial components of disturbance velocity, $\hat{p}$ is the disturbance pressure, α and n are the (real) axial and (integer) azimuthal wavenumbers and ω is

the complex eigenvalue. For a base flow with velocity field of the form $[0, 0, W(r)]$, eliminating the pressure from the disturbance momentum equations yields 3 equations for u, v and w:

$$D_* u + \frac{nv}{r} + \alpha w = 0, \tag{6}$$

$$\left[\gamma - \frac{i}{Re}\left(\alpha^2 + \frac{n^2}{r^2} - DD_*\right)\right]\zeta - \frac{2in}{r^3 Re}\eta + (W'u)' + \gamma' w = 0, \tag{7}$$

$$\left[\gamma - \frac{i}{Re}\left(\alpha^2 + \frac{n^2}{r^2} - D_* D\right)\right]\eta - \frac{2i\alpha}{Re}\xi - nW'u = 0, \tag{8}$$

where $D(\cdot) = (\cdot)' = d(\cdot)/dr$ and $D_* = D + 1/r$, Re is the Reynolds number based on pipe radius and centerline velocity[b], $\zeta = \alpha u + w'$, $\eta = \alpha r v - nw$ and $\xi = nu/r + D_* v$ are proportional to the azimuthal, radial and disturbance vorticity components and $\gamma = \alpha W - \omega$ is the term containing the eigenvalue which arises from the material derivative. While the above form suggests writing the equations entirely in terms of the disturbance vorticity components, this results in no practical simplification, as the manipulations required to rewrite the remaining u, v and w-terms in the equations entirely in terms of ζ, η and ξ rapidly become unwieldy. (In the code, these quantities are of course kept in terms of u, v and w). We further use (6) to eliminate w from (7) and (8), which yields a system of two equations, fourth and third-order, respectively, in the radial and azimuthal disturbance velocities u and v. The primitive-variable formulation has the advantage that it generalizes easily to a variety of base flow profiles, including (with the addition of the appropriate terms) ones with swirl. The only additional thing that is needed is a sufficient number of boundary conditions to make the sytem well-posed. For axisymmetric nonswirling flow in a circular pipe of radius R, the following hold:

$$r = 0: \begin{cases} |n| \neq 1: u, u'', v, v'' = 0 \\ |n| = 1: u', u''', v', v''' = 0, \end{cases} \qquad r = R: \; u, u', v = 0.$$

These give a sufficient number of boundary conditions, but note that for bending waves ($|n| = 1$,) the higher-order inner boundary condition on v involves a derivative of the same order at which this variable appears in the system. To remedy this, we rewrite the two (u, v)-disturbance equations in terms of two new dependent variables, ru and rv, for which the highest-order inner boundary conditions are reduced in order by one, and the lower-order inner and outer conditions are unaffected. The reformulated disturbance equations are discretized via Chebyshev collocation on a roots grid

[b] In the experiments, Re is based on diameter and average velocity; for the paraboloidal Poiseuille-flow velocity profile, these definitions are equivalent.

using sets of recombined basis functions which satisfy the requisite boundary conditions identically. As we have found the available software packages for solving general matrix eigensystems of the form $\mathbf{Ax} = \omega\mathbf{Bx}$ to be somewhat unreliable in terms of numerical quality, we first reduce the problem to one of standard form $\tilde{\mathbf{A}}\mathbf{x} = \omega\mathbf{x}$ by careful diagonalization of the B matrix and then find the eigenvalues using a complex QR-algorithm[c].

A key part of the non-modal analysis involves forming the matrix $\mathrm{M}(t)$ of discrete inner products, whose (j,k)th element is a weighted L^2 inner product of the jth and kth eigenfunctions:

$$\mathrm{M}_{jk}(t) = \langle \mathbf{u}_j, \mathbf{u}_k \rangle := e^{-i(\omega_j + \overline{\omega}_k)t} \int_0^R [u_j \overline{u}_k + v_j \overline{v}_k + w_j \overline{w}_k] r dr, \qquad j,k = 1,\ldots,m, \tag{9}$$

where m is the number of eigenfunctions retained in the expansion and the overbars denote complex conjugation. The individual eigenfunctions are normalized to have unity energy norm at time zero, that is,

$$\|\mathbf{u}_j(\cdot,0)\|^2 = \langle \mathbf{u}_j(\cdot,0), \mathbf{u}_j(\cdot,0) \rangle = \int_0^R [|u_j|^2 + |v_j|^2 + |w_j|^2] r dr = 1. \tag{10}$$

For details regarding the estimation of the possible amplification of energy density of an arbitrary initial disturbance, we refer the reader to the discussion in [7]; the only modification in the present case is that in order to estimate amplitude growth for comparison with the experiment, we define an amplitude growth function $A(t)$, which is simply the square root of the disturbance energy growth function $G(t)$ defined in equation (8) of Schmid & Henningson [7].

It is illuminating to visualize the inner products matrix, which (along with the eigenvalues) contains all of the information regarding non-normality of the m-mode approximation to the full linear evolution operator. We do this by using a single character to represent each element $\mathrm{M}_{jk}(0)$ of the time-zero inner products matrix. If the element has complex magnitude on the order of unity (specifically, $0.1 < |\mathrm{M}_{jk}| \leq 1$,) indicating that the two eigenfunctions in question are highly non-orthogonal, we use a zero to denote the element; if $0.01 < |\mathrm{M}_{jk}| \leq 0.1$, indicating that the eigenfunctions are weakly non-orthogonal, we use a one, and elements $|\mathrm{M}_{jk}| \leq 0.01$ (the eigenfunctions are essentially orthogonal) are represented simply with a dot. For instance, for the nonaxisymmetric- disturbance case having $n = 1$, $\alpha = 1.12$ and $Re = 7600$, the inner products ma-

[c]The code was checked by comparing the eigenvalues for $Re = 3000$ and $\alpha = 1$ against those tabulated for the same parameter values in [7]; the two sets of results were in complete agreement. The accumulation of round-off error in the computations increases rapidly with Reynolds number and disturbance wavenumbers (both α and n) and in all cases where the convergence, especially of the higher modes, became marginal, the results were checked using 128-bit real arithmetic.

trix, based on the 80 most-unstable modes and using the above representation, appears in Figure 3. (The inner products matrices for higher azimuthal wavenumbers look qualitatively similar.) Were this a normal operator, M(0) would simply be the identity matrix, and we would have a single row of symbolic zeros along the diagonal and dots elsewhere. In the above case, the thick band of zeros about the diagonal, especially near upper left, makes clear that the operator in question is highly non-normal – the amplitude growth function for this set of parameters (which represents the amplitude achievable from the particular combination of eigenmodes which maximizes non-modal energy growth at any given time[d]) grows by a factor of more than seventeen before beginning to decay, as it must at large time, since all of the individual eigenmodes are damped. The bandwidth is greatest between rows and columns 15 to 30, which correspond to the intersection of the three well-known branches of the spectrum in the complex plane, and this is where the largest contribution to the transient growth occurs. The classically least-damped modes contribute far less to the non-modal growth, as indicated by the smaller fraction of non-negligible inner products in the extreme upper left portion of the matrix, and the bandwidth decreases for increasingly more-damped modes, as well. The latter fact, along with the fact that the damping rates increase rapidly for the higher modes, causes the growth function to quickly asymptote to a limiting value as additional more-damped modes below the three-branch intersection point are included in the analysis[e].

Plots of the m-mode approximation to the amplitude growth function (with m sufficiently large to give at least four-figure convergence of $A(t)$ at all times) for cases with $Re = 7600$ and at the two axial wavenumbers $\alpha = 1.12$ and $\alpha = 1.75$, corresponding to the experimental cases at 10 Hz and 15 Hz appear in Figures 4 and 5, each for selected azimuthal wavenumbers ranging from 0 to 12. Analogous plots of energy growth have appeared elsewhere, but we include the amplitude plots for two reasons. First, the amplitude growth potential for the first few nonaxisymmetric mode families is rather larger than for the axisymmetric one, but only by roughly one order of magnitude, as

[d]Note that for a given set of wavenumbers α and n, the corresponding function $A(t)$ is an *envelope* curve, in that it represents the largest possible amplitude growth at any time t, maximized over *all* possible initial conditions consisting of a superposition of eigenmodes having those axial and azimuthal wavenmubers; thus, the initial states (as defined by the coefficients of their eigenfunction expansions) yielding the maximum amplitude growth at different times may not be the same. This is appropriate for the present study since the spatial structure, in particular with respect to the radial direction, of the initial disturbance field is not known with sufficient precision to prefer one particular initial state, i.e. set of expansion coefficients, over another.

[e]For axisymmetric modes, the (u, w) (torsional) and v (meridional) components of the vector eigenfunctions decouple, allowing the inner products matrix to be written in block diagonal form, each of the diagonal blocks qualitatively resembling Fig. 3. In this case, if both kinds of modes are present in roughly equal quantities, the transient growth is due entirely to non-orthogonality among the (u, w) modes, which is analogous to the decoupled Orr-Sommerfeld/Squire system, where the maximum non-modal growth is due entirely to the O-S modes.

opposed to two or more when one is measuring energy growth. Second, the envelope of transient growth (plotted for azimuthal wavenumbers $n = 0$, 1, 2, 3, 6 and 12 in each figure) reaches a maximum around $n = 3$, after which the maximum amplitude growth becomess progressively smaller. This would seem to imply that modes with $n = 1$, 2 and 3 are more important than those with $n = 0$, 6 and 12, but it must be remembered that $A(t)$ measures the maximum possible amplitude growth *relative to the initial amplitude* of the optimal non-modal disturbance in each case. Thus, if the experimental conditions are designed to suppress non-axisymmetry of the initial disturbance state, then the transient growth will be dominantly axisymmetric, even though the amplitude *ratio* for the optimally growing axisymmetric disturbance is relatively modest. In the experiment in question, the design is such that any possible transient disturbance growth will be dominated by modes with azimuthal wavenumbers which are integer multiples of six, in a proportion given by expression (4), which gives the estimated Fourier series coefficients of these modal families in the experiment in question. Finally, while the transient growth of nonaxisymmetric disturbances (i.e. $A(t)$ at any given $n \neq 0$) decreases as the disturbance wavelength decreases, the axisymmetric-mode transient growth increases from $\max_{0 \leq t < \infty}(A) = 3.48$ at $\alpha = 1.12$ to $\max_{0 \leq t < \infty}(A) = 3.88$ at $\alpha = 1.75$, indicating that the axisymmetric disturbance modes become more significant as the axial wavelength of disturbances decreases.

To compare with the experimental traces, we calculate the composite amplitude growth function,

$$A_{comp}(t) = c_0 A^0(t) + c_6 A^6(t) + c_{12} A^{12}(t) + \ldots, \tag{11}$$

where we use the superscripts to denote the azimuthal wavenumber of the mode family in question. The one-term-truncated (i.e. axisymmetric mode only, with the coefficient c_0 renormalized to unity) and three-term-truncated (with c_0, c_6 and c_{12} renormalized to sum to unity) composite amplitude growth functions corresponding to the two experimental cases are plotted as a function of down-stream distance in Figures 1 and 2, along with the experimental traces of disturbance amplitude, reproduced from Kaskel's paper. For the 10 Hz case, the experimental disturbance amplitude grows and decays somewhat more slowly than predicted by the non-modal analysis, but the maximum observed amplitude growth of just over a factor of four is in excellent agreement with the theoretical prediction, especially when the $n = 6$ and $n = 12$ modal families are included in the analysis. Further, the higher the frequency, the sooner and steeper the decay phase sets in, in consonance with the experiment: for the 15 Hz disturbance, both the observed rate of growth and decay and

the maximum amplitude are in good agreement with the theory.

Since the experiment in question was performed nearly thirty years before detailed theoretical predictions of the potential for non-modal growth in circular-pipe flow became available, there could be no sensitivity on the part of the experimenter to the quantitative factors involved in transient growth. We are therefore indeed grateful for the data traces included in Kaskel's report and believe on the basis of the arguments and calculations presented herein that these records depict transient growth in Poiseuille pipe flow. Besides being of interest from a historical perspective, the study in question also demonstrates an important aspect of the non-modal theory, namely that in the context of controlled or forced initial disturbance fields, non-modal growth estimates must take into account the relative initial sizes of the various components of the initial disturbance state.

Notes and Acknowledgements

We would like to thank Peter Schmid for helpful discussions during the preparation of this paper. All computations were performed on a DEC Alpha AXP 3000 workstation.

References

[1] A. Kaskel, "Experimental study of the stability of pipe flow. II. Development of disturbance generator", Tech. Report No. 32-138, Jet Propulsion Laboratory, Calif. Inst. of Tech., 1961.

[2] L. Boberg and U. Brosa, "Onset of turbulence in a pipe", *Z. Naturforsch.*, vol. 43a, pp. 697–726, 1988.

[3] K. M. Butler and B. F. Farrell, "Three-dimensional optimal perturbations in viscous shear flow", *Phys. Fluids*, vol. A4, pp. 1637–1650, 1992.

[4] L. N. Trefethen, A. E. Trefethen, S. C. Reddy, and T. A. Driscoll, "Hydrodynamic stability without eigenvalues", *Science*, vol. **261**, pp. 578–584, 1993.

[5] D. S. Henningson, A. Lundbladh, and A. V. Johansson, "A mechanism for bypass transition from localized disturbances in wall-bounded shear flows", *J. Fluid Mech.*, vol. **250**, pp. 169–207, 1993.

[6] S. C. Reddy and D. S. Henningson, "Energy growth in viscous channel flows", *J. Fluid Mech.*, vol. **252**, pp. 209–238, 1993.

[7] P. J. Schmid and D. S. Henningson, "Optimal energy density growth in Hagen–Poiseuille flow", *J. Fluid Mech.*, vol. **277**, pp. 197–225, 1994.

[8] B. G. B. Klingmann, "On transition due to three-dimensional disturbances in plane Poiseuille flow", *J. Fluid Mech.*, vol. **240**, pp. 167–195, 1992.

[9] L. Bergström, "Evolution of laminar disturbances in pipe Poiseuille flow", *Europ. J. of Mechanics B (Fluids)*, vol. **12** (6), pp. 749–768, 1993.

[10] L. Bergström, "Transient properties of a developing laminar disturbance in pipe Poiseuille flow", *Europ. J. of Mechanics B (Fluids)*, vol. 14 (5), pp. 601–615, 1995.

[11] P. L. O'Sullivan and K. S. Breuer, "Transient growth in circular pipe flow. I. linear disturbances", *Phys. Fluids*, vol. **6**, pp. 3643–3651, 1994.

[12] P. L. O'Sullivan and K. S. Breuer, "Transient growth in circular pipe flow. II. nonlinear development", *Phys. Fluids*, vol. **6**, pp. 3652–3664, 1994.

[13] L. Bergström, "Initial algebraic growth of small angular dependent disturbances in pipe Poiseuille flow", *Stud. Appl. Maths*, vol. **87**, pp. 61–79, 1992.

[14] L. Bergström, "Optimal growth of small disturbances in pipe Poiseuille flow", *Phys. Fluids*, vol. A **5** (11), pp. 2710–2720, 1993.

[15] L. Bergström, "Nonlinear behavior of transiently amplified disturbances in pipe Poiseuille flow", *Europ. J. of Mechanics B (Fluids)*, vol. 14 (6), pp. 719–735, 1995.

[16] E. Reshotko, "Experimental study of the stability of pipe flow. I. Development of an axially symmetric Poiseuille flow", Prog. Report No. 20-364, Jet Propulsion Laboratory, Calif. Inst. of Tech., 1958.

[17] D. S. Henningson and P. J. Schmid, "A note on measures of disturbance size for spatially evolving flows", *Phys. Fluids*, vol. **6**, pp. 2862–2864, 1994.

[18] D. M. Burridge and P. G. Drazin, "Comments on 'Stability of pipe Poiseuille flow"', *Phys. Fluids*, vol. **12**, pp. 264–265, 1969.

[19] E. W. Mayer and K. G. Powell, "Inviscid and viscous instabilities of a trailing line vortex", *J. Fluid Mech.*, vol. **245**, pp. 91–114, 1992.

Figure 1: Experimental traces and theoretical predictions of amplitude growth, F=10 Hz.

Figure 2: Experimental traces and theoretical predictions of amplitude growth, F=15 Hz.

Figure 3: 80-eigenfunction inner products matrix (symbolic form) for pipe flow at $Re = 7600$, $n = 1$ and $\alpha = 1.12$.

Figure 4: Nondimensional amplitude growth for pipe flow at $Re = 7600$, $\alpha = 1.12$ (F=10 Hz), at various azimuthal disturbance wavenumbers.

Figure 5: Nondimensional amplitude growth for pipe flow at $Re = 7600$, $\alpha = 1.75$ (F=15 Hz), at various azimuthal disturbance wavenumbers.

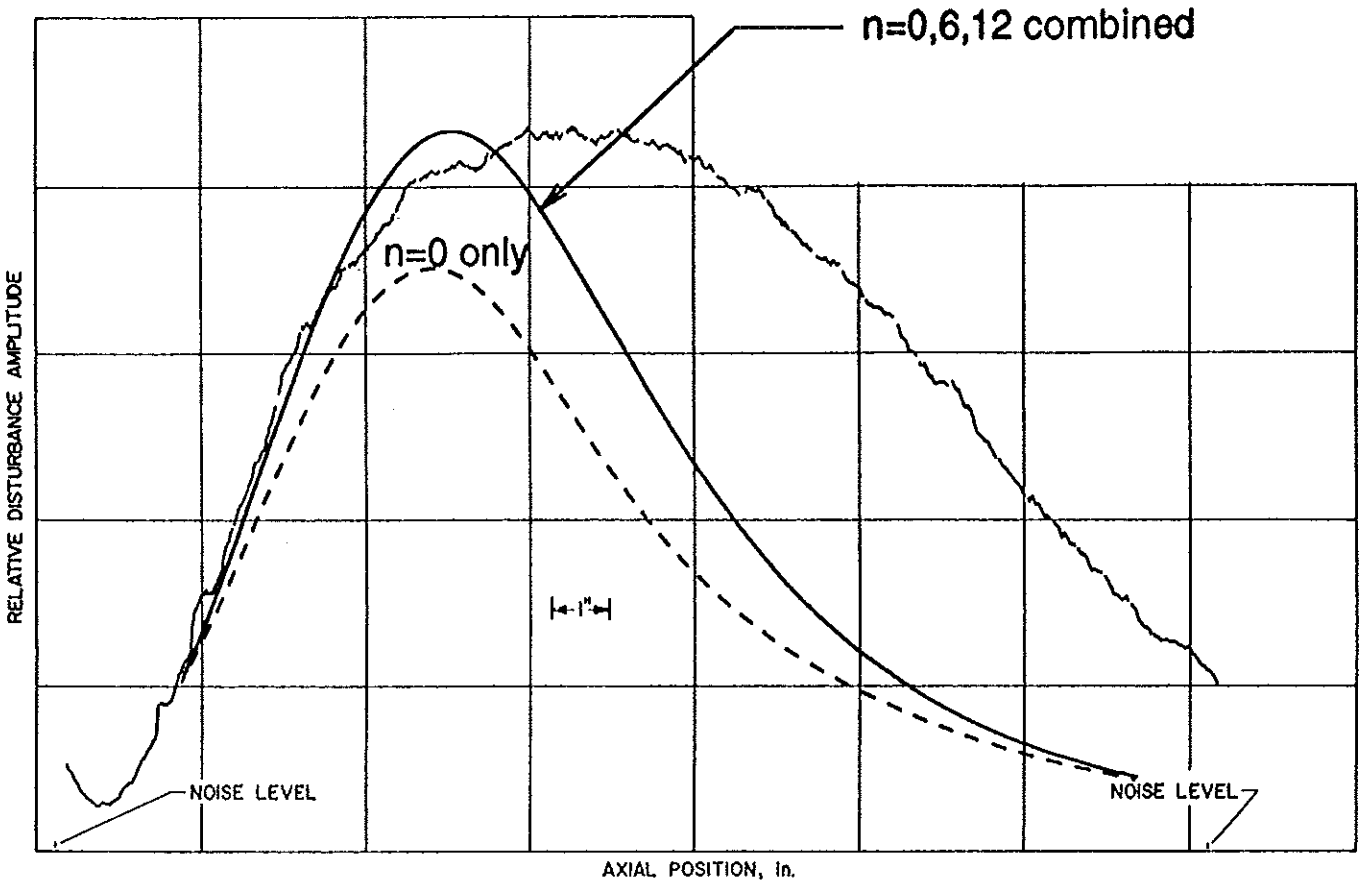
n=0,6,12 combined
n=0 only
RELATIVE DISTURBANCE AMPLITUDE
NOISE LEVEL
NOISE LEVEL
AXIAL POSITION, in.

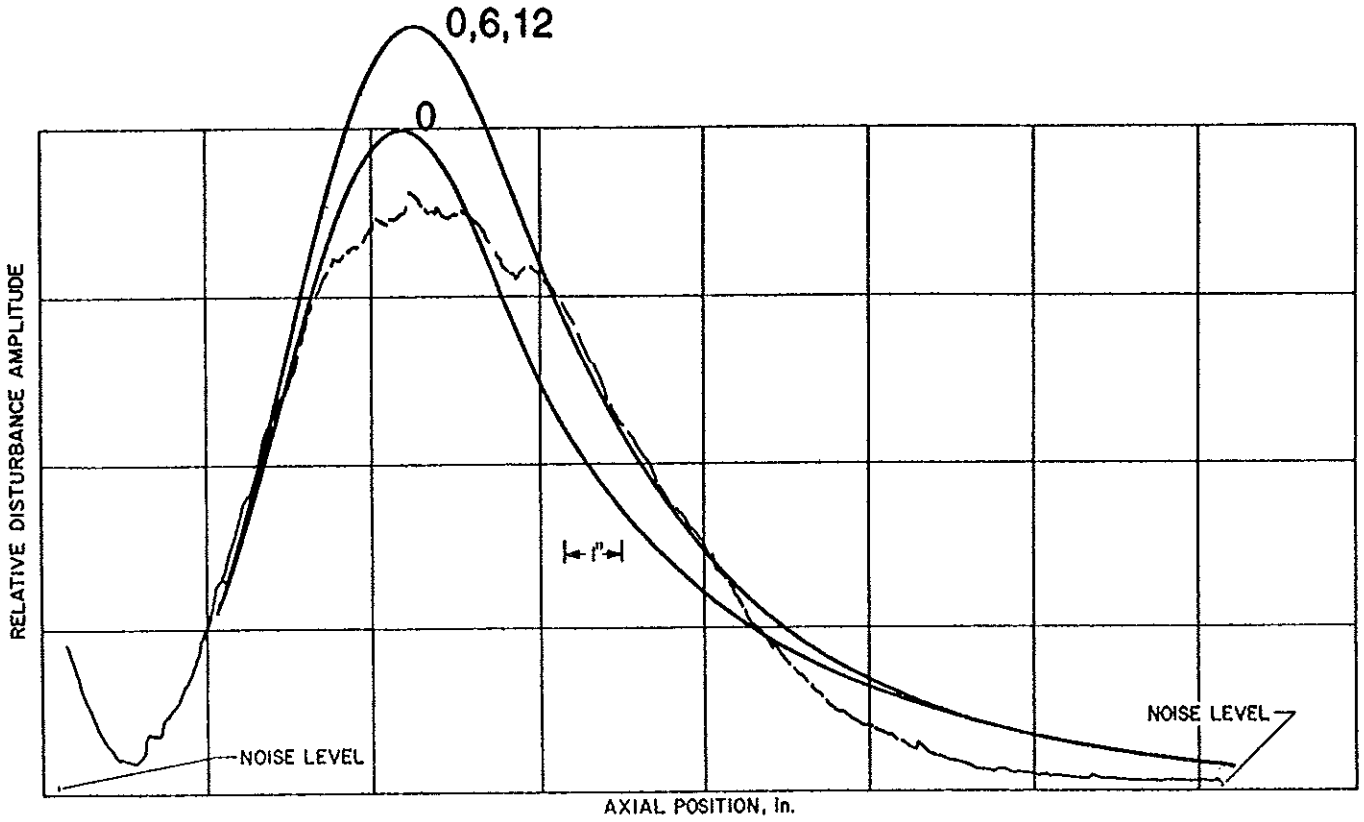
0,6,12
0
RELATIVE DISTURBANCE AMPLITUDE
1"
NOISE LEVEL
NOISE LEVEL
AXIAL POSITION, In.

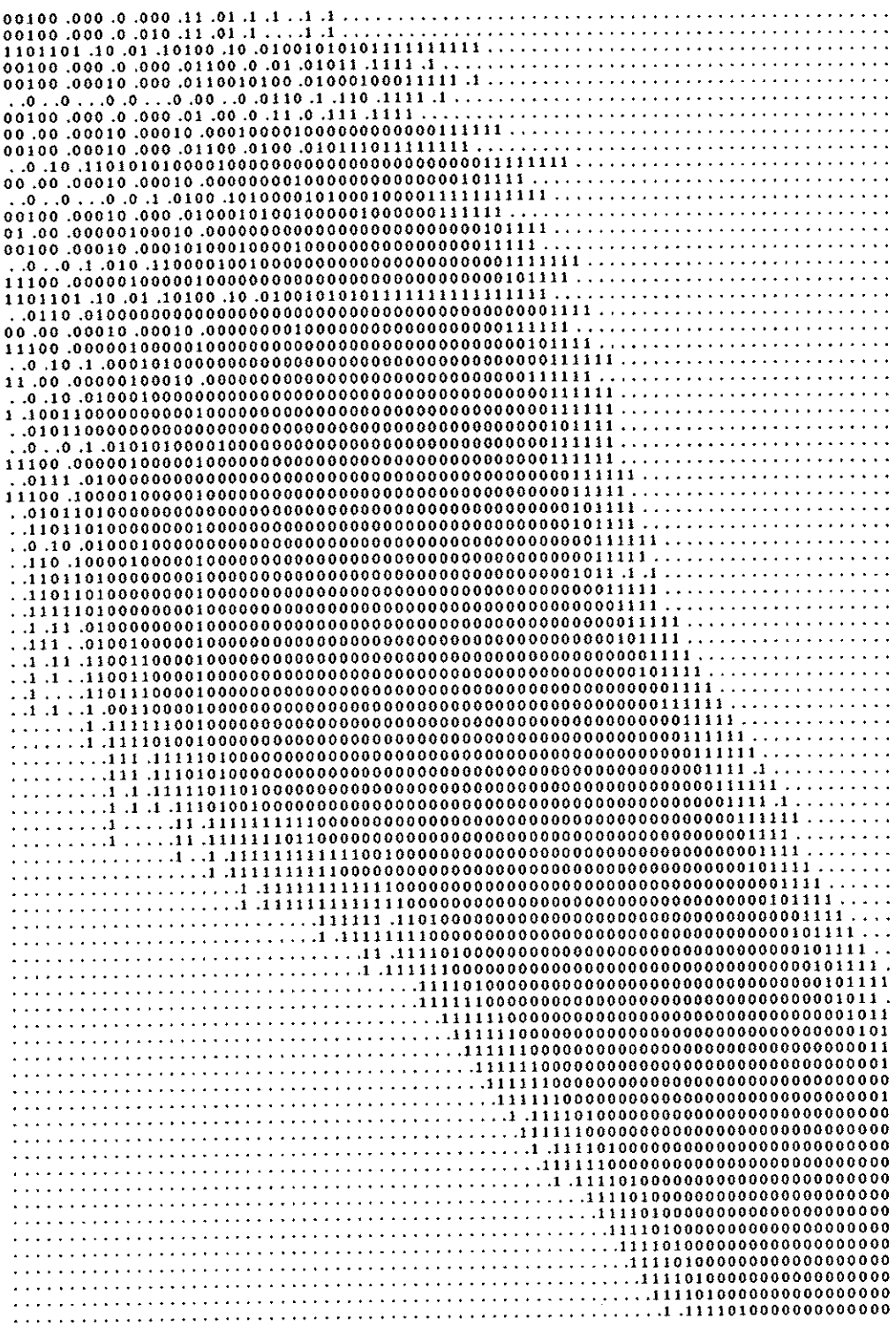

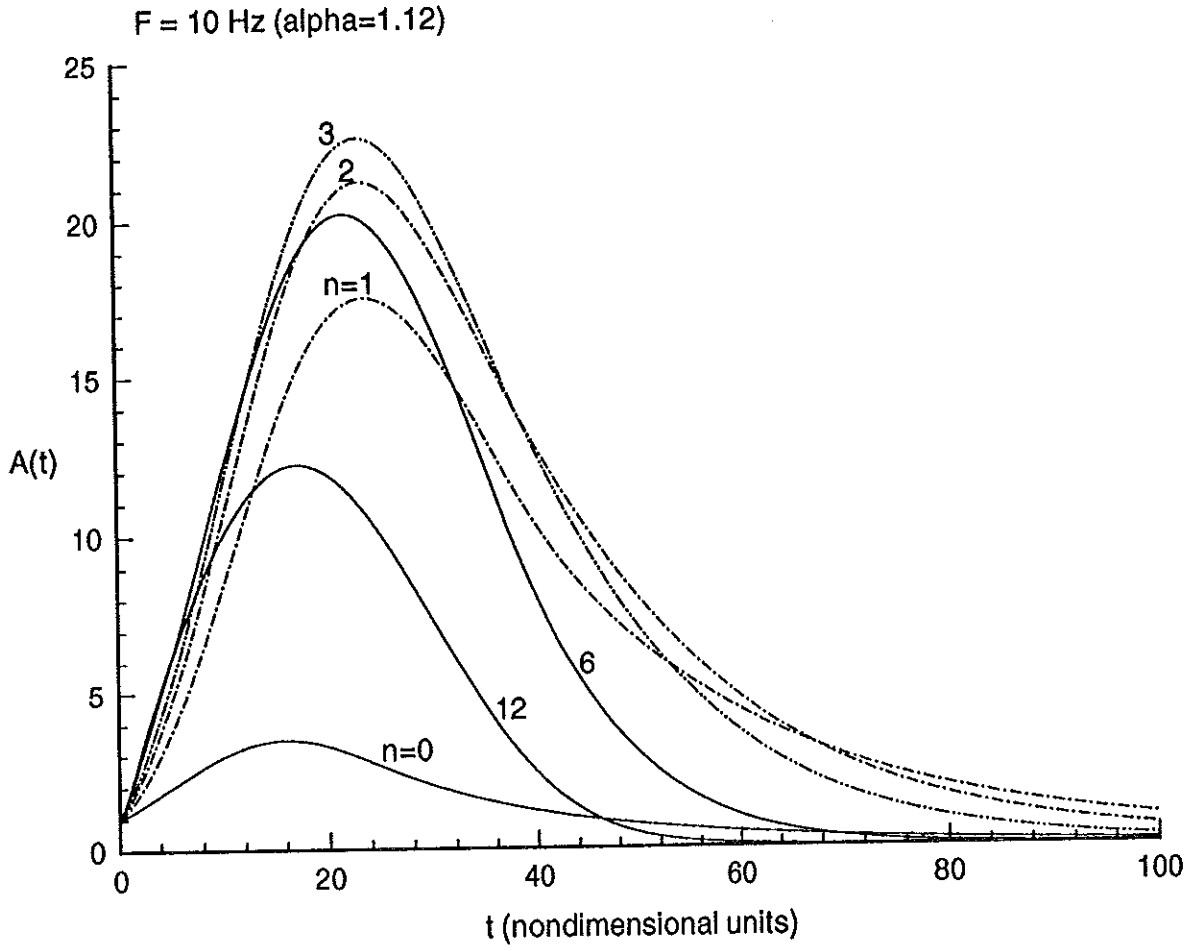

Figure 4: Nondimensional amplitude growth for pipe flow at $Re = 7600$, $\alpha = 1.12$ (F=10 Hz), at various azimuthal disturbance wavenumbers.

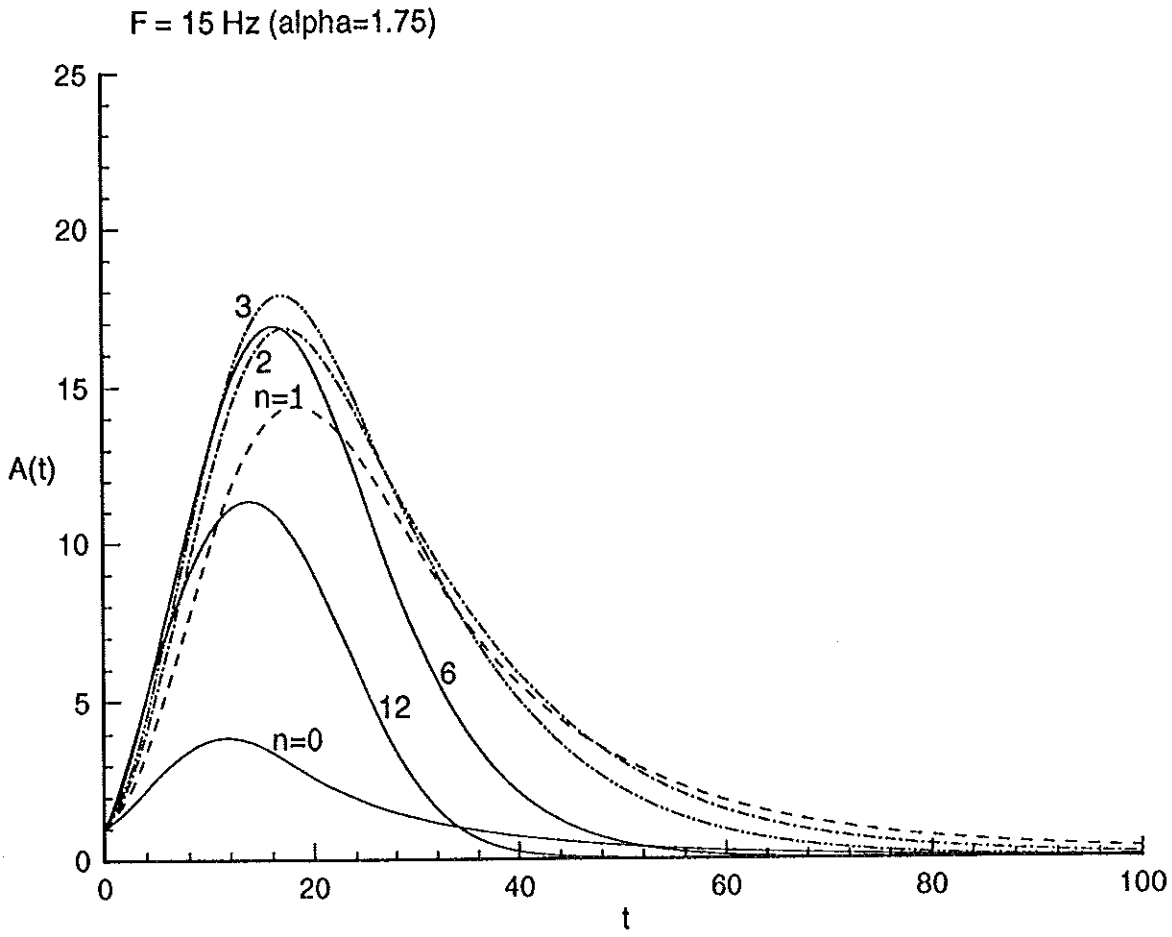

Figure 5: Nondimensional amplitude growth for pipe flow at $Re = 7600$, $\alpha = 1.75$ (F=15 Hz), at various azimuthal disturbance wavenumbers.